

Six-Phase Fully Coreless Axial-Flux Permanent-Magnet Generator: Design, Fabrication and Performance Analysis

T. Alsuwian¹, A. Habib², M.A.A. Mohd Zainuri^{2,3}, A. A. Ibrahim², Nasrudin Abd Rahim⁴, A.R.H. Alhawari¹, A.H.M. Almagani¹, S. Almasabi¹, A. T. Hindi¹, M. F. P. Mohamed⁵

¹ Electrical Engineering Department, College of Engineering, Najran University, Najran 66462, Kingdom of Saudi Arabia.

² Department of Electrical, Electronic and Systems Engineering, Faculty of Engineering and Built Environment, Universiti Kebangsaan Malaysia (UKM), Bangi, Malaysia.

³ Solar Energy Research Institute, Universiti Kebangsaan Malaysia (UKM), Bangi, Malaysia.

⁴ HICoE, UM Power Energy Dedicated Advanced Center (UMPEDAC), Wisma R&D, University of Malaya, 59990, Kuala Lumpur, Malaysia

⁵ School of Electrical and Electronics Engineering, Universiti Sains Malaysia, 14300 Nibong Tebal, Pulau Pinang

Corresponding author: M.A.A. Mohd Zainuri (e-mail: ammurrulatiqi@ukm.edu.my).

The authors express their gratitude for the support received from the Deputy for Research and Innovation at the Ministry of Education in the Kingdom of Saudi Arabia for this research, which was facilitated through a grant (NU/IFC/2/SERC/-/43) from the Institutional Funding Committee at Najran University, Kingdom of Saudi Arabia. Additionally, the authors acknowledge the contributions made by HICoE, UM Power Energy Dedicated Advanced Center (UMPEDAC), Wisma R&D, University of Malaya, Kuala Lumpur, Malaysia, for providing both software and certain components of the experimental setup, along with access to laboratory facilities.

ABSTRACT Coreless axial-flux permanent-magnet (AFPM) machines have recently gained prominence as efficient power generation solutions. Eliminating the core resolves challenges such as eddy current losses and cogging torque, enhancing overall efficiency. This topology enables high power density, further amplified in fully coreless configurations. Nevertheless, the proliferation of coreless AFPM machines faces hurdles as to high leakage flux and weaker structural integrity. Additionally, adopting multi-phase setups in AFPM introduces challenges, requiring additional winding coils and enlarging the stator diameter, leading to bulkier machine designs. This article underscores the significance of a lightweight, fully coreless six-phase machine and proposes a modular, multi-stage, multi-phase design tailored for fault-tolerant small-scale power generation applications. Furthermore, it explores the impact of employing double-layer winding coils on air-gap-flux density and power output. To realize this aim, a six-phase multi-stage AFPM generator was designed and simulated using ANSYS Maxwell®. Subsequently, a laboratory-scale prototype was fabricated accordingly. The simulation findings closely align with the experimental results obtained from the prototype, demonstrating the achievement of 1.3 kW power output. Notably, the six-phase machine with fully coreless concept exhibits a substantial power density of 205 W/kg. Multi-stage design boost efficiency and power density, presenting potential for small-scale applications

INDEX TERMS Coreless AFPM, MSMR topology, Six-phase prototype, High power-density.

I. INTRODUCTION

A coreless axial-flux permanent-magnet machine operates based on axial flux principles, but unlike traditional designs, it does not have an iron core in its stator. Instead, it utilizes non-ferrous materials or specialized configurations to support the windings and magnets. This coreless design provides several advantages, including reduced weight, high efficiency, increased power density, and improved cooling capabilities. In this machine, permanent magnets on the rotor and windings on the stator create electromagnetic fields, enabling the conversion between electrical and mechanical energy. The axial flux

configuration ensures efficient magnetic flux paths and optimal utilization of magnetic materials. These machines are valued for their compactness, high torque density, and adaptability across various applications, such as electric vehicles, renewable energy systems, robotics, and aerospace. Typically, stator and rotor are the two primary electromagnetic components for AFPM machines. However, the specific arrangement and number of these components can vary depending on the chosen topology. The literature documents a wide array of AFPM machine topologies, each with different implications for performance, size, and manufacturing ease [1]. These

topologies can generally be categorized into one of four [2] types: single-stator, single-rotor (SSSR); double-stator, single-rotor (DSSR); single-stator, double-rotor (SSDR); When comparing different types of AFPM (Axial-Flux Permanent-Magnet) machines, the MSMR (Multi-Stator Multi-Rotor) configuration is notable for its ability to produce high power and torque. This is due to its design, which allows for the stacking of multiple stators and rotors, enabling adjustments to power or torque as needed. This multistage setup boosts torque and power density without enlarging the machine's diameter. MSMR AFPM machines can be configured in various ways, such as slotted or slotless, with an iron core or coreless, and with NN or NS topologies, while maintaining consistent flux paths similar to their single-stage counterparts. Each architecture offers its own set of advantages and disadvantages based on its fundamental structure. Multistage AFPM machines are commonly used in applications like ship propulsion, medium range pumps, and low-speed generators. Similar to double-stage topologies like SSDR (Single-Stator Double-Rotor) or DSSR (Double-Stator Single-Rotor), MSMR machines can also be implemented in a coreless configuration, essentially representing a cascaded version of these designs. Additionally, a coreless architecture in MSMR machines can significantly enhance machine performance. Previous literature focused on only the stator as a coreless part of the machine for AFPM, but no one discussed fully coreless since for fully coreless there are some challenges to maintain the power [3, 4]. Because using non ferromagnetic material as rotor and stator allows magnetic flux leakage and in turns degrades the power[5]. The main target of this research is to achieve high power density by using fully coreless concept but at the same time ensure a high-power machine by cascading SSDR topology to make MSMR with some modification in the middle rotor and using of specific magnet configuration.

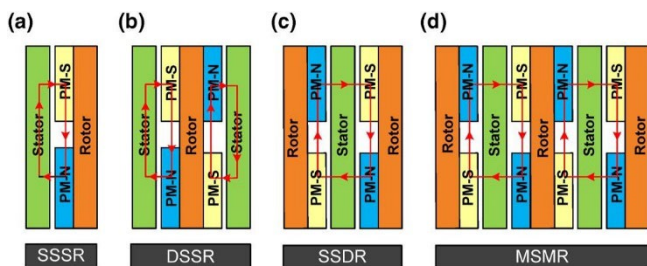


FIGURE 1. Schematics of various AFPM machine topology (a) single stator single rotor (SSSR), (b) double stator single rotor (DSSR), (c) single stator double rotor (SSDR), and (d) multiple stator multiple rotor (MSMR) [5]

Apart from that in recent years, in recent years, there has been a growing trend towards using multi-phase machines with higher phase counts, particularly in critical high-power applications. This shift is driven by the need for robust drive systems that deliver high performance while meeting strict reliability standards. [6]. Research efforts have focused on exploring the various benefits of this technology across different applications, each with specific phase requirements.

and multiple stator-multiple rotor (MSMR), as depicted in Fig 1.

Multi-phase machines offer several advantages over those with three-phase machine, although they require custom converter designs to handle their unique characteristics [7]. In contrast, more than three-phase winding designs can easily use commercially available three-phase power converters, making them more accessible for widespread use in industries such as automotive, aerospace, military, and nuclear, where high reliability is essential. For reliable solutions in industrial applications, multi-phase induction machines paired with multi-phase inverter drives are promising options. These systems typically have more than three phases on the stator side, necessitating a corresponding number of legs in the inverter [8]. This configuration provides several advantages, including improved power handling capabilities through power distribution across multiple phases, reduced torque fluctuations, and enhanced reliability. Notably, unlike traditional three-phase setups, the failure of one or more stator phases or inverter legs does not prevent the machine from starting and operating. Additionally, multi-phase systems offer increased torque per ampere for a given machine size, reduced stator copper losses, and lower rotor harmonic currents [9].

However, designing a multi-phase machines in axial flux configurations presents challenges due to the need for two-layer winding in axial-flux machines [10]. Increasing the number of phases leads to an increase in the number of winding coils, which in turn enlarges the diameter of the machine. Additionally, utilizing a double layer of winding coils can elevate the air-gap flux density, resulting in a reduction in power and torque output. Taking these demerits into account, multi-stage machine (MSMR AFPM) is used. In MSMR machines, multiple stators ensure a minimum air-gap flux density between rotors, which addresses the aforementioned bottleneck. This article ultimately aims to propose a design for a fully coreless MSMR (Multi-Stator Multi-Rotor) AFPM (Axial-Flux Permanent-Magnet) machine with six-phase windings, targeting high power density. This work's novelty lies in developing a fully coreless AFPM machine capable of delivering high power density. Six-phase windings concept is applied here leveraging the advantages of the multiple stators in an AFPM machine, as six-phase machines offer several benefits over conventional three-phase machines, as previously discussed.

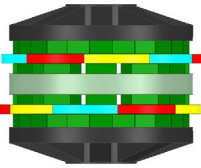
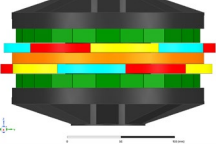
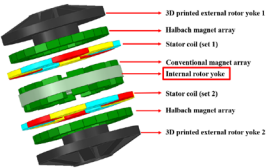
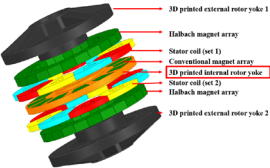
The paper is structured in the following manner: It begins with an introduction in the opening section. Moving forward, Section II explores the modeling process of a six-phase fully coreless AFPM. Section III then elaborates on the fabrication of a prototype for the six-phase fully coreless AFPM generator. Following this, Section IV conducts a comprehensive analysis of the results and performance obtained. Finally, Section V concludes the paper by

summarizing the key findings and providing closure to the discussion.

II. MODELING OF MSMR FULLY CORELESS AFPM GENERATOR

The multistage coreless AFPM generator can utilize either a double-stator single-rotor (DSSR) or a single-stator double-rotor (SSDR) configuration [11]. For a fully coreless design, the SSDR configuration is chosen, where an N-stage machine will have N stators and (N+1) rotors. In this research, a two-stage (N = 2) multi-stage machine is examined. The simplest form of a multistage coreless AFPM generator involves directly combining two or more single-stage or double-stage AFPM machines [12]. For example, merging two double-stage machines can easily create a multistage setup, enhancing torque or power output while maintaining the same machine size.

TABLE I
BASIC DIFFERENCE BETWEEN DIRECT AND CUSTOMIZED METHOD OF MULTI-STAGE CORELESS AFPM MACHINES

Direct method for multi-stage coreless AFPM	Modified method for multi-stage coreless AFPM
	
Complete model of the machine	Complete model of the machine
	
Different parts of the machine	Different parts of the machine

With two external rotors and one internal rotor (as detailed in Table I), the direct cascade multi-stage AFPM configuration generally comprises two stators and three rotors in total. The internal rotor, formed through direct cascading, effectively represents the back-to-back rotors of a double-stage generator. The stator coils consist of single-layer concentrated windings with a trapezoidal shape, embedded in epoxy and coated with a composite material hardener for mechanical strength. To achieve a fully coreless design and reduce weight, simple modifications have been made to enhance the machine's power density. Two key modifications differentiate the MSMR from the direct cascade multi-stage coreless AFPM generator:

- Halbach arrays are used on the 3D-printed external rotors to prevent flux leakage towards the machine's exterior.

- Instead of two internal rotors (back-to-back) one single 3D-printed internal rotor with a conventional magnet array is used for simplifying the design and conserving materials.

This modified MSMR topology is derived from the modular SSDR Halbach Epoxy rotor design. Analysis of the flux path shows that this new topology maintains a similar path to the direct cascade multi-stage coreless AFPM generator but is more compact and lightweight due to the elimination of the iron yoke from both the rotor and stator. The total volume of magnets in the internal and external rotors is balanced by adjusting the magnet thickness. Therefore, while the magnet thickness in the external disc rotors may differ from that in the internal rotors, the external rotors have a greater number of magnets compared to the internal ones. Figure 2 illustrates the differences between the external and internal rotors of the fully coreless multi-stage AFPM generator. The airgap is maintained at 0.5 mm on both sides of rotors and stators, and the average magnetic flux density (B_g) is measured in the mid-plane of the gap between each rotor and stator. A plane region for the MSMR is shown in Figure 3.

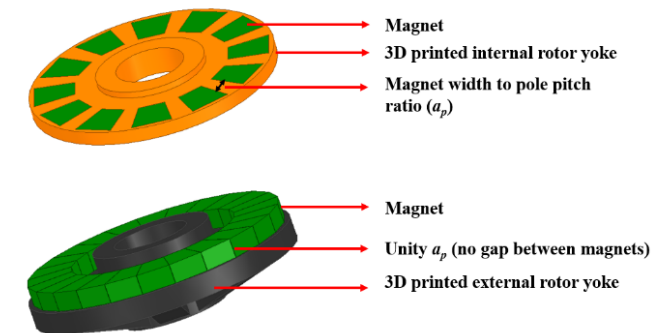


FIGURE 2. Diagram of Inner rotor and outer rotor

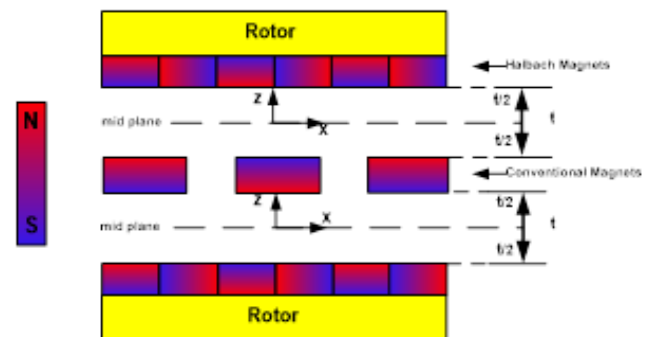


FIGURE 3. Plane region delineated for the multi-stage coreless AFPM generator. [13]

Furthermore, the stator coil's maximum current loading is predetermined to ensure safe operation of the machine. A stator current of 3 A is chosen in accordance with the stator wire gauge. Fig 4 illustrates the various load resistances for the

multi-stage coreless AFPM generator with a fixed current loading. The generator is configured with 12 poles (equivalent to 6 pole pairs) and 18 coils (9 coils per stator) to achieve a speed of 500 rpm at 50 Hz.

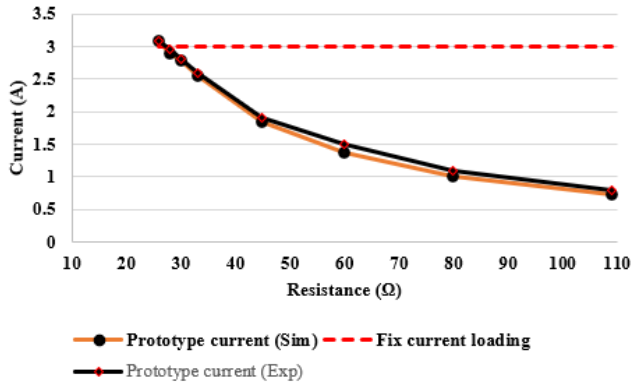


FIGURE 4. Fixed stator current loading for different load resistance

III. PROTOTYPE FABRICATION OF SIX-PHASE MSMR FULLY CORELESS AFPM GENERATOR

Using simulation models, a prototype of the MSMR AFPM generator has been carefully fabricated, leveraging the outcomes from FEA simulation models which have been cross-checked against physical results obtained from this prototype to ensure validation. The prototype machine represents an axial-flux permanent-magnet design utilizing ironless material, rendering it fully coreless. It features a configuration comprising three rotors and two stators. Fig 5 displays all the individual components of the machine. With a nominal power of 1.3 kW and a nominal rotational speed of 500 rpm, the machine employs Neodymium-Iron-Boron magnets (Grade: N45H). Trapezoidal-shaped magnets are securely adhered to the surface of the 3D-printed rotor disk made from nylon carbon fiber, known for its high heat resistance. Regarding the stator yoke material is also used nylon carbon fiber 3D filament.

TABLE II
IMPORTANT PARAMETER OF PROTOTYPE MACHINE

Parameter	Explanation	Value
P	Rated power	1.3 kW
n	Rated speed	500 rpm
T	Rated torque	30 Nm
I_{ph}	Rated phase current	3 A
l_{PM}	Thickness of PM	10 mm & 12.98 mm
B_{rs}	PM's remanence flux density	120 °C 1.34 T
H_{ci}	PM's intrinsic coercivity,	963 kA/m
V_{ph}	Rated phase voltage	220
Q	Number of stator coils	9/stator
p	Number of pole pairs	6
g	Length of the airgap per stator & rotor	0.5 mm
D_{out}	External dia of the stator stack	200 mm
D_{in}	Internal dia of the stator stack	85 mm
N_{coil}	Number of coils turns in series per phase	1050
G_{PM}	Total Mass of PM's	3.5 kg

The machine winding type is a conventional non-overlapping concentrated round wire winding coil for which the number of coils per pole and phase is equal to a fractional number. The key specification parameters of the machine are listed in Table II.

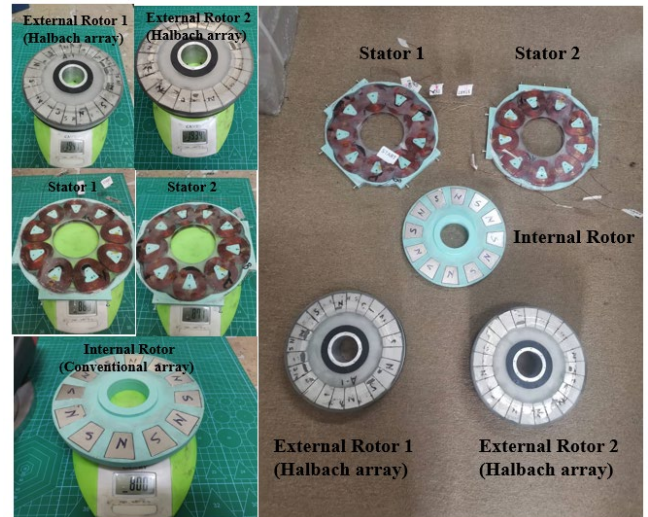


FIGURE 5. Weight specifications for various components of the prototype machine.

The external rotors, made with a 3D printed yoke as depicted in Fig 5, incorporate the Halbach magnet array. To strengthen the magnetic flux density, the necessity of placing Halbach magnets one after another, coupled with the non-ferromagnetic nature of the yoke, makes it challenging to easily position the magnets within the rotor yoke. Consequently, a high strength epoxy hardener is employed to securely affix the magnets in place within the rotor yoke. An aluminum hollow shaft (4 mm thick) is inserted to the middle of the yoke to make it easily installable to the main shaft with other parts of the machine. Conventional array magnets are embedded within the internal rotor to carry the magnetic flux density between the external rotor magnets. The rotor structure is also made with 3D printed yoke. The internal rotor yoke has an extended circular support ring on both sides of the rotor aiding to centrally neutralize the attraction force between the rotors magnets and fix a constant air-gap distance between the rotors. Both stators feature a 3D printed yoke housing trapezoidal coils embedded in high-temperature resistant epoxy. The stators coils (Fig 5) are wound in automatic winding machine ensured a compact and precise coil according to the FEA design. The coils are wound using AWG 24 wire with a diameter of 0.51 mm. The absence of cores in both rotors and stators results in minimal attraction force between rotors and stators. However, the prototype's robust mechanical structure effectively manages any residual attractive force between the stator and rotor disks. The number of coils per pole and per phase in the stator winding is less than 1 signifying a concentrated winding. Each of the phase coils includes 350 turns and the total number of phase turns is then 1050. Both ends of the phase windings of the stators are available in a connection box. This leads to the possibility of

changing the machine's electrical connection from a star to delta orientation, altering the connection between the stators from parallel to series, or operating the machine using only one stator. The two stators are connected in parallel, to operate the machine as a six-phase machine.

A. TEST RIG DESCRIPTION

An in-house designed and constructed test bench, as shown in Figure 6, has been developed for experimental purposes. This setup incorporates a 2.2 kW motor with a flange rating of 1400/72 rev/min, a torque transducer (MAGTROL Type: TMB 310/411) capable of measuring up to 50 N-m, and a 24-V DC power source to operate the generated prototype. Coupling bellows are installed to address any misalignments. Line-to-line voltages, phase currents, and torque are monitored using a Tektronix 4-channel digital storage oscilloscope. Four oscilloscopes are used to collect data for a six-phase machine, with each oscilloscope dedicated to capturing the voltage for three phases and the current for three phases, resulting in a total of six phases for voltage and current measurement. A 1.5 kW variable frequency drive motor controller is used to control the machine. To connect with the six-phase generator, a pair of three-phase resistive loads (as shown in Figure 6) are used to create a six-phase load.

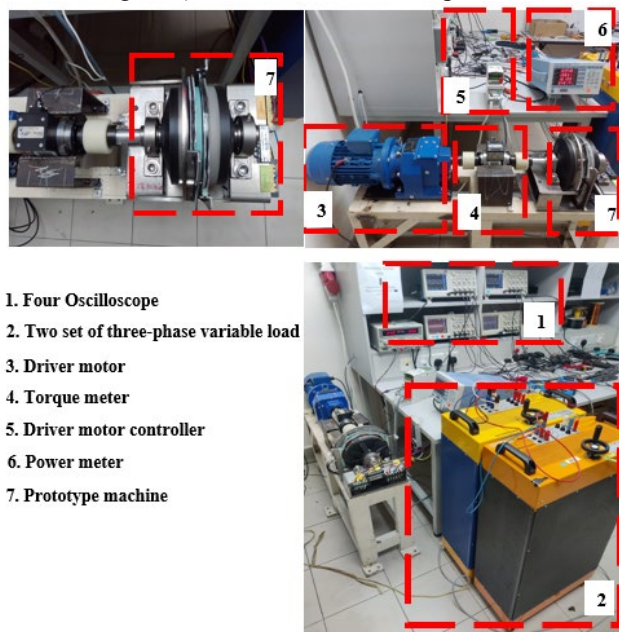


FIGURE 6. Prototype test set-up

Additionally, when determining the generator's total weight, only the active components of the materials were taken into account. Advanced 3D printing techniques were utilized during manufacturing, along with epoxy hardener to reduce overall weight. Consequently, the prototype generator has achieved a remarkably low weight of 6.42 kg.

B. SIX-PHASE WINDING CONNECTION

In many practical applications, six-phase configurations with varying angular displacements between the two sets of three-phase windings have been widely studied due to their appeal. [7]. Mainly three types of winding configurations of six-phase are familiar. They are dual three-phase (D3P), symmetrical six-phase (S6P), and asymmetrical six-phase (A6P) [3]. However, in this research the machine is equipped to function in S6P configurations. In S6P each phase has an equal 60 electrical degrees phase shift. Fig 7 illustrates 3 familiar possible configurations for six-phase.

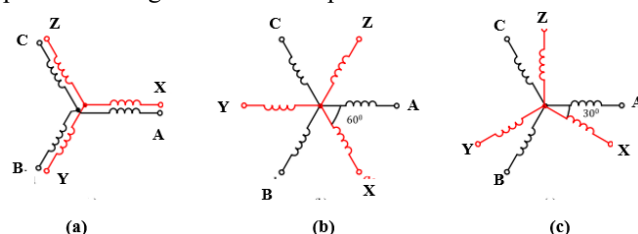


FIGURE 7. Possible windings configuration for 6 phase (a) D3P, (b) S6P and (c) A6P

The machine utilizes a six-phase stator, consisting of 2 sets of 3 phases, along with a customizable terminal box. This allows for the comparison of various twelve-terminal configurations (comprising 6 phases and 6 neutrals) by reconfiguring the stator terminals. This approach enables the attainment of an equivalent six-phase stator while maintaining consistent stator machine dimensions and copper volume across all connections. However, since six-phase has two groups of three-phase stator windings: the ABC group (stator-1) and the XYZ group (stator-2). In the prototype machine there one stator is fixed (say 1st stator) where another stator (2nd stator) can be rotated mechanically. Mechanical 0-degree, 5-degree and 10-degree rotation applied to get electrical 0-degree, 30-degree and 60-degree phase displacement. For S6P all the end ports of the windings like A2, B2, C2, X2, Y2, Z2 are connected in one neutral point, while other six ports (A1, B1, C1, X1, Y1, Z1) are connected to the load, only the 2nd stator is shifted 60 degrees (electrical). Fig 8 showing the connection diagram of S6P, while Fig 9 shows the equivalent circuit of the load connection.

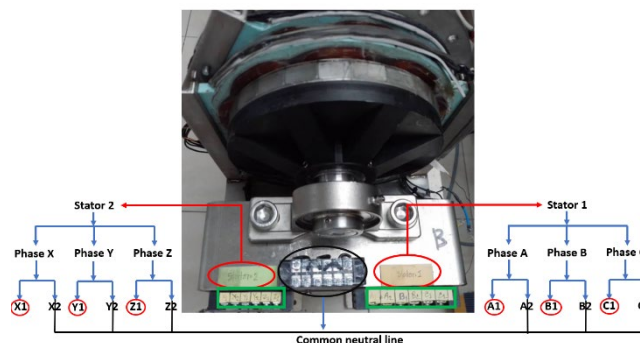


FIGURE 8. Physical stator connection for S6P.

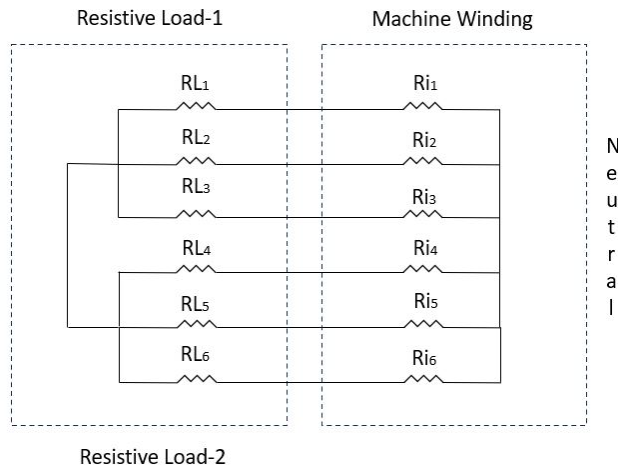


FIGURE 9. Equivalent circuit of load connection.

IV. PERFORMANCE ANALYSIS OF SIX-PHASE MSMR FULLY CORELESS AFPM GENERATOR

The test begins with an open circuit voltage test to analyze the windings' characteristics. Following this, a six-phase load—comprising two sets of three-phase load banks—is applied to the machine, which is then operated under varying current loads and speeds to evaluate its dynamic performance. A comparison between the simulation and experimental results reveals a minimal difference. Figures 10, 11, and 12 display the voltage, current, and torque for both the prototype and simulation results. Notably, the prototype exhibits less torque ripple compared to the simulation. This reduction in torque ripple is attributed to an internal low-pass filter within the torque meter, which attenuates most of the torque ripples. Consequently, the waveform is smoothed, resulting in the observation of minimal torque ripples.

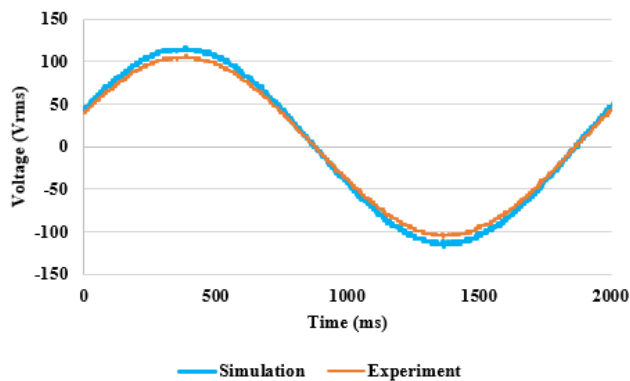


FIGURE 10. Open circuit voltage comparison for simulation and experiment for S6P

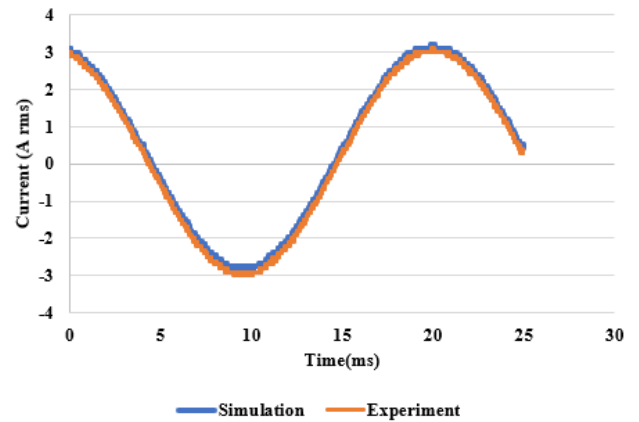


FIGURE 11. Current comparison for simulation and experiment for S6P

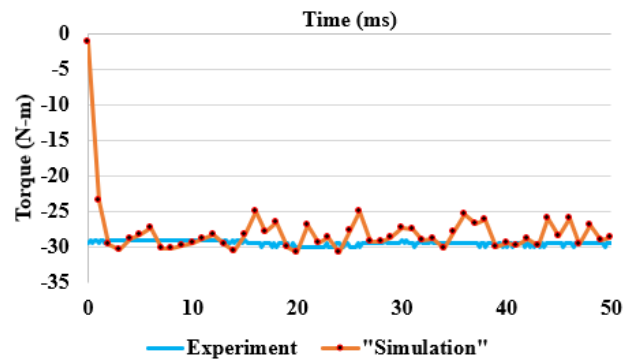


FIGURE 12. Torque comparison for simulation and experiment for S6P

Comparison between experimental and simulation results is made for the open circuit voltage, closed circuit current, and torque at 500 rpm. Both sets of values closely align, with the open circuit voltage being 113 V and the current 3 A. However, there is a discrepancy in torque ripple: the experimental average torque is 30 N-m with a 4% ripple, whereas the simulated torque shows a higher ripple of 17%. The reduced torque ripple in the experimental results is attributed to the filtering effect discussed in the initial paragraph of Section IV. Despite this, only the experimental results are presented for the dynamic test, as the key output parameters have already been validated by the simulation results.

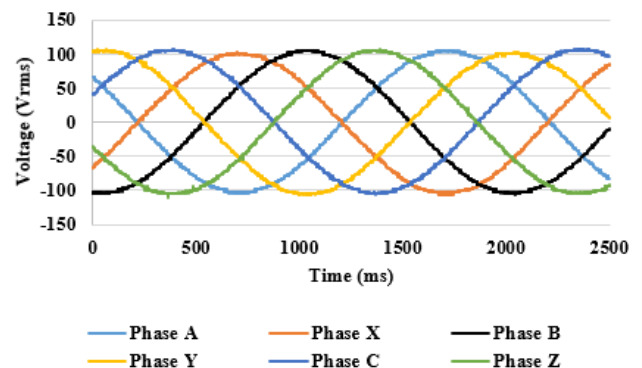


FIGURE 13. Open circuit voltage for S6P

The smooth winding flux distribution due to the 60-degree electrical phase shift leads to a slightly higher voltage. Fig. 13 shows the complete open circuit voltage characteristics of the S6P (experimental). Additionally, at a fixed current load, different load resistances are applied to the machine running at a rated speed of 500 rpm to achieve the rated current, as previously illustrated in Figure 4 of Section II.

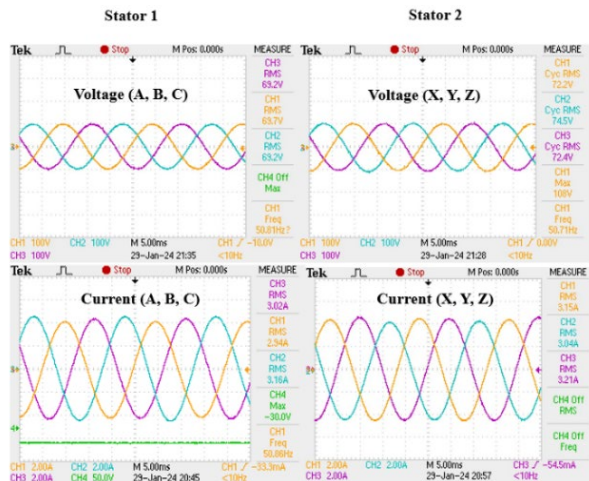


FIGURE 14. Voltage, current and torque in loaded condition for S6P

Under loaded conditions, it's common for voltage to drop while current rises. However, the data from Fig. 14 shows an average voltage of 71.2 V and an average current of 3.08 A, while producing a mechanical torque of 30 N-m. The dynamic operation reveals a slight linear increase in both torque and current, maintaining a parallel gap, which indicates the machine's consistent and healthy operation across different speeds. As the speed varies, there is a marked linear increase in voltage, suggesting evenly distributed flux linkage to the stator windings. This relationship between voltage, current, and torque with speed variation is shown in Fig. 15, while Fig. 16 illustrates the variations in power and efficiency.

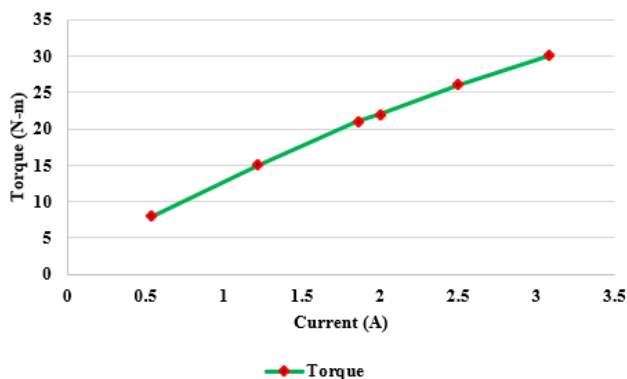


FIGURE 15. Voltage, current and torque relation with changing of speed for S6P

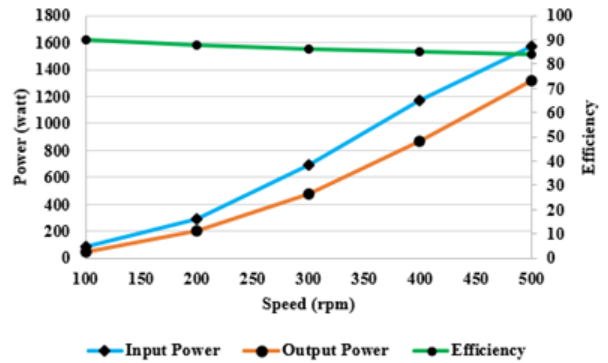


FIGURE 16. Power and efficiency plot for S6P

Fig. 17 illustrates a clear link between speed and power, affirming that higher speeds lead to greater power generation. At 500 rpm rated speed, the generator achieves a maximum power of 1315 W, confirming this direct correlation between speed and power. Meanwhile, Fig. 18 displays the relationship between torque and current, demonstrating a linear trend that suggests torque performance improves as current levels rise. This consistency with anticipated behavior suggests that increasing current levels result in higher torque output.

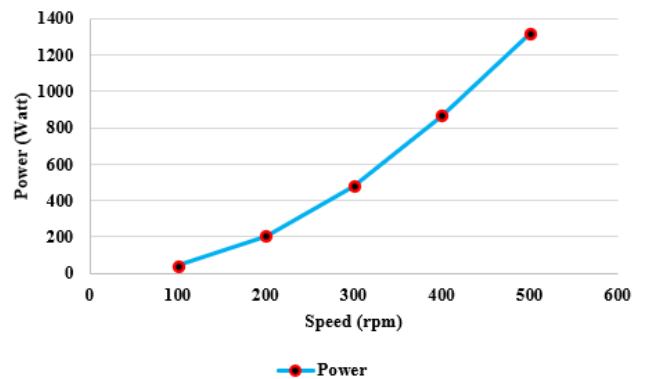


FIGURE 17. Power vs. speed plot

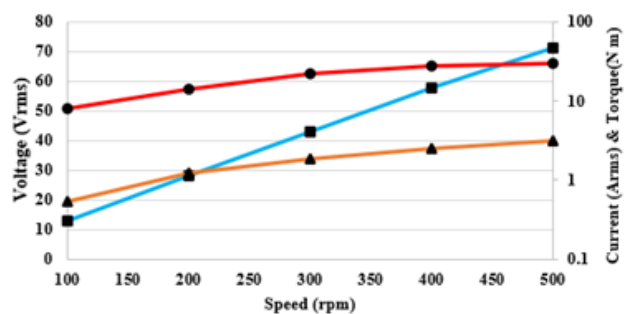


FIGURE 18. Torque vs. current plot

V. CONCLUSION

A novel prototype of a six-phase fully coreless MSMR AFPM generator has been constructed and its performance has been verified against simulation results. The comparative analysis

demonstrated close alignment between the performance of the constructed machines and the simulated outcomes. However, at the rated operating conditions, the generator provided 1.3 kW of power with 30 N-m of torque. Despite a relatively lower efficiency due to increased copper loss from multiple stators in the multi-stage configuration, notable achievements in power density were observed. The study's key findings reveal several significant outcomes. Firstly, the fully coreless design notably enhanced power density, reaching an impressive 205 W/kg. Moreover, employing the fully coreless concept enabled the generator to yield a substantial power output of 1315 kW, utilizing a cascading multi-stage topology. The implementation of a six-phase system in multi-stage AFPM was found to be straightforward, offering the advantage of utilizing multiple stator coils. However, despite these advantages, the generator's efficiency measured at 83.8% was deemed unsatisfactory for a fully coreless generator, primarily due to the considerable number of coils causing high copper loss. As a result, the recommended design approach for MSMR initially suggests using the minimum required number of stator coils, with the possibility of interconnecting these basic units to achieve high power in subsequent stages.

ACKNOWLEDGMENT

The authors express their gratitude for the support received from the Deputy for Research and Innovation at the Ministry of Education in the Kingdom of Saudi Arabia for this research, which was facilitated through a grant (NU/IFC/2/SERC/-/43) from the Institutional Funding Committee at Najran University, Kingdom of Saudi Arabia and also from University Kebangsaan Malaysia Grant under GUP-2022-024.

REFERENCES

1. Shao, L., et al., *Design and Construction of Axial-Flux Permanent Magnet Motors for Electric Propulsion Applications—A Review*. IEEE Access, 2021.
2. Mahmoudi, A., et al., *Axial-flux permanent-magnet machine modeling, design, simulation, and analysis*. 2011. **6**(12): p. 2525-2549.
3. Pirzad, S., et al., *Optimal mixed control of Axial Flux Permanent Magnet Synchronous generator wind turbines with modular stator structure*. ISA Transactions, 2021.
4. Khan, S., S.S.H. Bukhari, and J.S. Ro, *Design and Analysis of a 4-kW Two-Stack Coreless Axial Flux Permanent Magnet Synchronous Machine for Low-Speed Applications*. Ieee Access, 2019. **7**: p. 173848-173854.
5. Habib, A., et al., *A systematic review on current research and developments on coreless axial-flux permanent-magnet machines*. IET Electric Power Applications, 2022. **16**(10): p. 1095-1116.
6. Subotic, I., et al., *Isolated chargers for EVs incorporating six-phase machines*. IEEE Transactions on Industrial Electronics, 2015. **63**(1): p. 653-664.
7. Abdel-Khalik, A.S., M.S. Abdel-Majeed, and S. Ahmed, *Effect of winding configuration on six-phase induction machine parameters and performance*. IEEE Access, 2020. **8**: p. 223009-223020.
8. Abdel-Khalik, A.S., A.M. Massoud, and S. Ahmed, *An improved torque density pseudo six-phase induction machine using a quadruple three-phase stator winding*. IEEE Transactions on Industrial Electronics, 2019. **67**(3): p. 1855-1866.
9. Abdel-Khalik, A.S., A. Massoud, and S. Ahmed, *Standard three-phase stator frames for multiphase machines of prime-phase order: Optimal selection of slot/pole combination*. IEEE Access, 2019. **7**: p. 78239-78259.
10. Buksnaitis, J.J., *Six-Phase Electric Machines*. 2018: Springer.
11. Caricchi, F., et al., *Multistage axial-flux PM machine for wheel direct drive*. IEEE Transactions on Industry Applications, 1996. **32**(4): p. 882-888.
12. Kahourzade, S., et al., *A comprehensive review of axial-flux permanent-magnet machines*. 2014. **37**(1): p. 19-33.
13. Habib, A., et al., *A fully coreless Multi-Stator Multi-Rotor (MSMR) AFPM generator with combination of conventional and Halbach magnet arrays*. 2020. **59**(2): p. 589-600.



TURKI M. ALSUWIAN was awarded a B.Sc. degree in Electrical Engineering from King Saud University, Riyadh, Saudi Arabia. He worked as an electrical power engineer in a Saudi Electricity Company from April 2004 until January 2009. In 2011, he received an M.Sc. degree in Electrical Engineering from Gannon University, Pennsylvania State, USA. In 2018, he obtained a Ph.D. degree in Electrical Engineering from the University of Dayton, Ohio State, USA. Currently, he is an

Associate Professor in the Electrical Engineering Department, Najran University, Saudi Arabia. His main research interests are applied control in different fields such as flight control, power quality control, power electronics control, communication control, adaptive control, modeling control, artificial intelligence, and smart grids.



ASIFUL HABIB academic journey began with a B.Sc. (Hons.) from Ahsanullah University of Science & Technology, Dhaka, Bangladesh, in 2009. He pursued an M.Sc. at the University of Malaya, Kuala Lumpur, Malaysia, in 2020, and completed his Ph.D. at Universiti Kebangsaan Malaysia (UKM), Bangi, Selangor, in 2024. Currently a Research Assistant in the Department of Electrical, Electronic, and System Engineering at UKM, Asiful has also contributed significantly to the UM Power Energy Dedicated

Advanced Centre (UMPEDAC) at the University of Malaya. His research interests include electrical machine design, solar PV and wind technologies, electric vehicles, and renewable energy applications. Asiful's work continues to push the boundaries of technology and sustainability.



MUHAMMAD AMMIRRUL ATIQI MOHD ZAINURI was born in Kuala Lumpur, Malaysia in 1988. He received the Bachelor degree in Electrical and Electronic Engineering in 2011, MSc (Electrical Power Engineering) in 2013 and Doctorate Ph.D (Electrical Power Engineering) in 2017 from Universiti Putra Malaysia. He is currently Senior Lecturer at Department of Electrical, Electronic and Systems Engineering, Faculty of Engineering and Built Environment, Universiti Kebangsaan Malaysia, Selangor, Malaysia. His areas of research interests are power electronic, power quality, microgrid, renewable energy system and electrical vehicle.



AHMAD ASRUL IBRAHIM is currently a senior lecturer in the Department of Electrical, Electronic and Systems Engineering, Universiti Kebangsaan Malaysia. He received the BEng and MSc degrees from Universiti Kebangsaan Malaysia, Bangi, Malaysia and the PhD degree from Durham University, Durham, United Kingdom in 2008, 2012 and 2018, respectively. His research interests are distribution system automation, artificial intelligence, renewable energy integrations, power quality assessment, demand side management and smart systems.



NASRUDIN ABD. RAHIM received the B.Sc. (Hons.) and M.Sc. degrees from the University of Strathclyde, Glasgow, U.K., and the Ph.D. degree from Heriot-Watt University, Edinburgh, U.K., in 1995. He is currently a Professor with the University of Malaya, Kuala Lumpur, Malaysia, where he is also the Director of the UM Power Energy Dedicated Advanced Centre (UMPEDAC). He is also a Distinguish Adjunct Professor with the Renewable Energy Research Group, King Abdulaziz University, Jeddah, Saudi Arabia. His research interests include power electronics, solar PV and wind technologies, real-time control systems, and electrical drives. He is a Fellow of the Institution of Engineering and Technology, U.K. and the Academy of Sciences Malaysia. He is also a Chartered Engineer, U.K.



ADAM R. H. ALHAWARI was born in Irbid, Jordan. In 2003, he was awarded a B.Sc. degree in Communication Engineering by Hijjawi Faculty for Engineering Technology at Yarmouk University, Jordan. He obtained both postgraduate degree of M.Sc. and Ph.D. degrees in 2009 and 2012, respectively, in Wireless Communications Engineering from Universiti Putra Malaysia. Previously, he started the entry level with the post of senior lecturer in Universiti Putra Malaysia from 2012 to 2015. Currently, he is a professor in the department of Electrical Engineering at Najran University, Kingdom of Saudi Arabia. His main research interests are microstrip filters, metamaterials, antenna systems, ultra-wideband imaging, wireless biosensors, and RFID.



ABDULKAREM H. M. ALMAWGANI graduated his B.Sc. in Information Engineering from the College of Engineering in Baghdad University in 2003. He was awarded the M.Sc. in Electronic Systems Design Engineering and Ph.D. in Communication Engineering from Universiti Sains Malaysia, in 2008 and 2011, respectively. He was an Assistant Professor in the Electrical Engineering Department, Faculty of Engineering, University of Science and Technology, Sana'a, Yemen, until February 2014 when he moved to Najran University.

Currently, he is an Associate Professor position in the Electrical Engineering Department, College of Engineering, Najran University, Saudi Arabia. His main research interests are signal-processing algorithms with application to telecommunications and wireless communication networks.



SALEH ALMASABI received the B.S. degree in electrical and electronics engineering from the King Fahd University of Petroleum and Minerals (KFUPM), Saudi Arabia, in 2008, the M.S. degree from Wayne State University, Detroit, MI, USA, in 2014, and the PhD degree from Michigan State University, East Lansing, MI. He is currently an Assistant Professor with the Electrical Engineering Department, Najran University Saudi Arabia. His research interests include power systems, smart grids, reliability, PMU applications, and cyber physical security.



A. T. HINDI was born in Jordan. He received his B.S. in Electrical Engineering from Vinnitsa Technical University in 1995 and PhD degree in Power Systems Engineering from Vinnitsa Technical University in 2004. Currently he is an assistance professor at the Electrical Engineering department, Najran University, Saudi Arabia. His main research interests include compensation of reactive power energy and consumption in electric installation and systems.



MOHAMED FAUZI PACKEER MOHAMED received the B.Eng. degree in Electrical and Electronics Engineering (with distinction) from Universiti Tenaga Nasional (UNITEN) in Kajang, Selangor, Malaysia in 2002. He obtained the M.Sc. degree in Electronics System Design Engineering from Universiti Sains Malaysia (USM) in Nibong Tebal, Pulau Pinang in 2010, and a Ph.D. degree in Electrical and Electronics Engineering from The University of Manchester (UoM) in Manchester, United Kingdom in 2015. He joined the School of Electrical and Electronics Engineering at Universiti Sains Malaysia (USM) as a Senior Lecturer. Prior to joining the university, he gained 7 years of industrial experience from 2002 to 2009 in semiconductor wafer fabrication and packaging. His current research interests include simulation, design, fabrication, and characterization of high RF and high-power devices based on compound semiconductor materials. He is also keen on the research area of Organic Thin Film Transistors and GaN HEMT.